Electronic Supporting Information

for

Oxidation-State-Controlled Switching Between AIE and ACQ in Pyrene Luminophores

Vignesh Rajendran[a], K. R. Justin Thomas[a*]

[a]Organic Material Laboratory, Department of Chemistry, Indian Institute of Technology Roorkee, Roorkee, 247667, India.

* Corresponding author: krjt@cy.iitr.ac.in

Table of contents

	Instrumentation	**S3**
	Experimental section	**S4**
	Density Functional Theory (DFT) calculations	**S4**
	Crystallization methods	**S5**
	Synthesis and experimental procedures	**S6-S8**
	Photophysical studies	**S9**
Fig. S1	(a) Emission spectrum of all dyes in (a) thin film (b) solid.	**S9**
Table S1	Summary of photophysical properties	**S9**
Fig. S2	Lifetime decay of all dyes in solution, thin film and solid.	**S10**
Table S2	Lifetime decay of all dyes in solution, thin film and solid.	**S10**
Fig. S3	Decomposed Hirshfeld surface plots of **DS blue** showing contributions from (a) C···C, (b) C···H, and (c) S···H interactions.	**S11**
Fig. S4	Decomposed Hirshfeld surface plots of **DS green** showing contributions from (a) C···C, (b) C···H, and (c) S···H interactions	**S11**
Fig. S5	Decomposed Hirshfeld surface plots of **DS (1)** showing contributions from (a) C···C, (b) C···H, and (c) S···H interactions	**S11**
Fig. S6	Decomposed Hirshfeld surface plots of **DSO** showing contributions from (a) C···C, (b) C···H, (c) S···H, and (d) O···H interactions.	**S12**
Fig. S7	Decomposed Hirshfeld surface plots of **DSO_2** showing contributions from (a) C···C, (b) C···H, and (c) O···H interactions.	**S12**
Fig. S8	(a) Absorption, (b) emission spectra of **DS** recorded in different solvents.	**S12**
Fig. S9	(a) Absorption, (b) emission spectra of **DSO** recorded in different solvents.	**S13**
Fig. S10	(a) Absorption, (b) emission spectra of **DSO_2** recorded in different solvents	**S13**
Table S3	Solvatochromic data of **DS** in various solvents.	**S13**
Table S4	Solvatochromic data of **DSO** in various solvents.	**S13**
Table S5	Solvatochromic data of **DSO_2** in various solvents.	**S14**

Table S6	Solvatochromic properties of all dyes.	**S14**
Fig. S11	AIE study of (a) **DS** and (b) **DSO_2** in THF/H_2O mixture.	**S14**
Fig. S12	(a) I/I_0 plot of **DS** and **DSO_2** (b) Lifetime decay of (b) **DS** (c) **DSO** in aggregated fractions.	**S15**
Table S7	Selected bond lengths and angles observed in **DS**, **DSO** and **DSO_2**	**S15**
Fig. S13	Noncovalent interactions analysis of (a) **DS_{b1},** (b) **DS_{b1},** (c) **DS_g** crystals	**S16**
Fig. S14	Emission spectrum of mechanochromic behaviour of **DS_g** crystal (λ_{ex} = 370 nm).	**S16**
Fig. S15	Lifetime decay of all the (a) **DS_{b1}, DS_{b1}, DS_g** (b) **DS_g ground**	**S17**
Table S8	Kinetic parameter of (a) **DS_{b1},** (b) **DS_{b1},** (c) **DS_g** crystals	**S17**
Fig. S16	Noncovalent interactions analysis of (a) **DSO** (b) **DSO_2**	**S17**
Fig. S17	Frontier molecular orbital energy level of all dyes.	**S18**
Fig. S18	FMOs HOMO/HOMO-1 and LUMO/LUMO+1 electronic distributions and difference density plot for S_1 state of all dyes.	**S18**
Fig. S19	(a) Cyclic voltammetry and (b) DPV of all dyes recorded in DCM	**S19**
Fig. S20	Thermal stability of all dyes	**S19**
Table S9	Thermal and electrochemical properties of all dyes	**S19**
Table S10	Kinetic parameter of all dyes in various water fractions	**S20**
Fig. S21	SEM images of all dyes	**S20**
Fig. S22	Concentration dependent emission of (a) **DS**, (b) **DSO**, and (c) **DSO_2**	**S21**
Table S11	Crystal data and structure refinement for **DSb_1**	**S21**
Table S12	Crystal data and structure refinement for **DS_{b2}**	**S22**
Table S13	Crystal data and structure refinement for **DS_g**	**S22**
Table S14	Crystal data and structure refinement for **DSO**	**S23**
Table S15	Crystal data and structure refinement for **DSO_2**	**S24**
Fig. S23	^{1}H NMR (500 MHz, $CDCl_3$*D*) of (**2**)	**S25**
Fig. S24	^{1}H NMR (500 MHz, $CDCl_3$) of **DS**	**S25**
Fig. S25	^{13}C NMR (126 MHz, $CDCl_3$) of **DS**	**S26**
Fig. S26	^{1}H NMR (500 MHz, $CDCl_3$) of **DSO**	**S26**
Fig. S27	^{13}C NMR (126 MHz, $CDCl_3$) of **DSO**	**S27**
Fig. S28	^{1}H NMR (500 MHz, $CDCl_3$) of **DSO_2**	**S27**
Fig. S29	^{13}C NMR (126 MHz, $CDCl_3$) of **DSO_2**	**S28**
	References	**S28**

Instrumentation

The ^{1}H and ^{13}C NMR spectra were recorded in a JEOL 500 MHz spectrometer instrument at 298 K with $CDCl_3$ as a deuterated solvent and TMS as an internal standard. Chemical shifts (δ) are reported in ppm relative to residual solvent signals $CDCl_3$: 7.26 ppm for ^{1}H NMR and 77.10 ppm for ^{13}C NMR. HRMS spectra were acquired on Agilent Mass Hunter Qualitative Analysis 10 Software. UV-Vis absorption spectra for all the final dyes were recorded on a Cary 100 UV-vis spectrophotometer. Fluorescence emission spectra have been recorded in the Horiba Scientific Fluoromax 4C spectrophotometer. The dyes' absolute photoluminescence quantum yield (PLQY) was determined by the calibrated integrating sphere method in the Edinburgh spectrofluorometer. The fluorescence lifetime measurements of liquid, solid, and thin film samples, including fitting, were acquired by the FLS 1000 Edinburgh instrument. FE-SEM Carl Zeiss Ultra Plus was acquired to study the morphology of aggregated samples. All data were collected from a single crystal at 103 K on a Bruker D8 QUEST FIXED CHI diffractometer with a microfocus sealed tube using a multilayer mirror as monochromator and a Bruker PHOTON III CPAD detector. The diffractometer was equipped with an Oxford Cryostream 1000 low temperature device and used Mo K_α radiation (λ = 0.71073 Å). All data were integrated with SAINT V8.42, yielding 36530 reflections of which 4943 where independent (average redundancy 7.39) and 74.0% were greater than $2\sigma(F^2)$. A Multi-Scan absorption correction using SADABS 2016/2 was applied. The structure was solved by Intrinsic Phasing methods with SHELXT 2018/2 and refined by full-matrix least-squares methods against F^2 using SHELXL-2019/2. All non-hydrogen atoms were refined with anisotropic displacement parameters. All hydrogen atoms were refined isotropic on calculated positions using a riding model with their U_{iso} values constrained to 1.5 times the U_{eq} of their pivot atoms for terminal sp^3 carbon atoms and 1.2 times for all other carbon atoms. An electrochemical analyzer with a three-electrode set up (glassy carbon as working electrode,

non- aqueous $Ag/AgNO_3$ as reference electrode, and platinum auxiliary electrode) was used to record cyclic voltammetry (CV) and differential pulse voltammetry (DPV) with ferrocene as internal standard and tetrabutylammonium perchlorate as supporting electrolyte using BASi Epsilon electrochemical analyzer. The thermal stability of dyes was observed by thermogravimetric analysis (TGA) using a Perkin–Elmer Pyris diamond analyzer instrument with a heating rate of 10°C/min and by maintaining a nitrogen atmosphere.

Materials

All the required chemicals were purchased from the available commercial sources and used without further purification. Pyrene, *p*-toluene thiol, *m*CPBA, Cs_2CO_3, all other reagents and solvents were purchased and utilized without further purification from Sigma Aldrich, TCI, and SRL chemicals. All the solvents were distilled using the appropriate distillation set up for further studies. Precoated alumina plates from Merck grade were used for thin layer chromatography (TLC) analysis. All the compounds were purified using column chromatography over silica gel having mesh sizes ranging from 200-400.

Experimental section

Density Functional Theoretical Calculations

All the theoretical calculations were performed using ORCA 6.0.1 software[1] at the B3LYP/def2-svp level. The geometries of the lowest excited singlet (S_1) and triplet (T_1) states were optimized by TD-DFT. The global minima of the optimized structures were confirmed by frequency calculation on the optimized structures which showed no negative frequencies. TD-DFT calculations at the B3LYP/def2-tzvp level on the optimized structures were performed to estimate the excitation energies, singlet-triplet energy gap and other relevant parameters. Natural transition orbitals (NTO) and the charge transfer indices were calculated using a Multiwfn program.[2]

Crystallization procedure

All the crystal was obtained by solvent vapor diffusion technique. For this, **DS_{b1}, DS_{b2}** and **DS_g** crystalized using different solvent mixtures like DCM/Hexane, THF/Hexane and DCM/MeOH, whereas **DSO** and **DSO_2** crystal obtained by DCM/Hexane layering at room temperature.

Excited state dipole moment and Lippert Mataga plot calculations

In this equation, $\mu_e - \mu_g$ the dipole moments in the ground and excited states, respectively, h is Planck's constant, c is speed of light, a is radius of molecules and Δv is Stokes shift, which is calculated from the difference between absorption and emission maxima in the wave number scale (cm^{-1}). The Lippert-Mataga plot for **DS, DSO, and DSO_2** dyes having Stokes shift (Δn cm^{-1}) plotted against orientation polarizability (ε) and Lippert-Mataga solvent polarity parameters (n) and Δf (ε, n) has been calculated from Eq. (1). The Δf orientation polarizability is expressed in Eq. (2) as

$$\Delta v = \vartheta_{abs} - \vartheta_{emi} = \frac{2(\mu_e - \mu_g)^2}{hca^3}\Delta f + Cont \qquad (1)$$

$$\Delta f(\varepsilon,n) = \left(\frac{(\varepsilon - 1)}{(2\varepsilon + 1)} - \frac{(n^2 - 1)}{(2n^2 + 1)}\right) \qquad (2)$$

Where Δf is orientation polarizability, ε and n are solvent dielectric constant and refractive index respectively and Δv for Stokes shift.[3]

Synthesis procedures

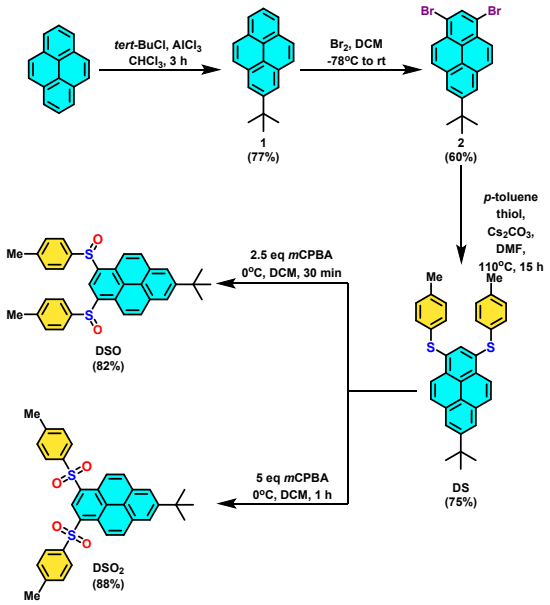

Scheme 1 Synthetic route of all three dyes.

Synthesis of precursors: 1

1 was synthesized by following reported protocol.[4] In a 250 mL RB flask, compound pyrene (25 g, 123 mmol) was dissolved in dry DCM (100 mL) and cooled at 0 °C. Afterward, $AlCl_3$ (16.5 g, 123 mmol, 1 equiv.) was added in one portion at the same temperature. Finally, dropwise *t*-BuCl (13.4 mL, 123 mmol, 1 eq) was added to the mixture under N_2 atm. Then, the brown mixture was shifted to room temperature and allowed to stir for 3 hours. After completing reaction hours, excess of $AlCl_3$ was quenched by adding sat. $NaHCO_3$ solution. Then, the organic phase was extracted with DCM, dried over anhydrous sodium sulfate, and concentrated by rotary evaporation. Finally, the crude product was purified by column chromatography (eluant: 100% Hexane) and obtained as colourless solid having a 77% yield. ^{1}H NMR (500 MHz, $CDCl_3$) δ 8.44 (s, 1H), 8.34 (d, J = 9.2 Hz, 2H), 8.29 (s, 2H), 8.16 (d, J = 9.2 Hz, 2H), 1.60 (s, 11H).

Synthesis of precursors: 2

2 was synthesized by following reported protocol.[5] To a flask tert-butyl pyrene (5 g, 19.35 mmol, 1 eq) in DCM (100 mL) was maintained at -78 °C. Afterward liq. Br_2 (1.9 mL, 38.97 mmol, 2 eq) in DCM (40 mL) was added dropwise to the mixture at same temperature. Then allowed to stir for 15 hours at room temperature. Next reaction mixture was quenched by sat. $Na_2S_2O_3$ solution (10 mL). The resultant precipitate was collected under vacuum and washed with methanol (40 mL). Finally crude product was washed with hexane (20 mL) which yield the white solid (4.83 g, 60% yield) and used without further purification. ^{1}H NMR (500 MHz, $CDCl_3$) δ 8.44 (s, 1H), 8.34 (d, J = 9.2 Hz, 2H), 8.29 (s, 2H), 8.16 (d, J = 9.2 Hz, 2H), 1.60 (s, 9H).

Synthesis of DS

In RB flask equipped with condenser (**1)** (1 g, 2.4 mmol, 1 eq), *p*-toluenethiol (655 mg, 5.20 mmol, 2.2 eq) and Cs_2CO_3 (1.7 g, 5.20 mmol, 2.2 eq) was dissolved in 15 mL of DMF followed by N_2 purging over 5 min. Then heated at 110 °C for 15 hours at N_2 atm. After cooling to room temperature mixture was poured into cold water and the precipitate was filtered and dried over vacuum. Finally crude product was purified by column chromatography using 5% $CHCl_3$/Hexane as eluent got pale green solid (907 mg, 75% yield). ^{1}H NMR (500 MHz, $CDCl_3$) δ 8.56 (d, *J* = 9.2 Hz, 2H), 8.24 (s, 2H), 8.10 (d, *J* = 9.2 Hz, 2H), 8.01 (s, 1H), 7.12 – 7.10 (m, 4H), 7.02 – 7.00 (m, 4H), 2.30 (s, 6H), 1.58 (s, 9H) ppm. ^{13}C{^{1}H} NMR (125 MHz, $CDCl_3$) δ 149.93, 136.70, 134.90, 132.67, 131.10, 130.18, 128.84, 125.95, 124.50, 123.33, 122.66, 35.34, 31.95 ppm. IR (KBr) cm^{-1}: 3040, 2946, 2916, 2859, 1586, 798, 713. HRMS: Calculated mass $C_{34}H_{31}S_2$ [$(M+H)^+$] 503.1861; found 503.1848.

Synthesis of DSO

A Ccompound **(2)** (250 mg, 0.49 mmol, 1 eq) was dissolved in 20 ml of DCM at 0 °C. Subsequently (55-60%, 422 mg, 2.45 mmol, 2.5 eq) *m*CPBA added slowly to the mixture was stirred at 0 °C for 1 hours. Next the organic layer washed with brine (30 mL) and dried over

anhydrous sodium sulphate. Then solvent was removed using rotary evaporation and crude product was purified by column chromatography using 50% DCM/Hexane as eluent gave green-yellow solid (209 mg, 82% yield). IR (KBr) cm^{-1}: 3040, 2922, 2917, 2852, 1592, 1081, 1055, 806. ^{1}H NMR (500 MHz, $CDCl_3$) δ 9.24 (s, 1H), 9.14 (s, 1H), 8.63 (dd, *J* = 9.2, 1.1 Hz, 2H), 8.58 (d, *J* = 9.2 Hz, 2H), 8.33 (d, *J* = 6.2 Hz, 4H), 8.22 (dd, *J* = 11.6, 9.2 Hz, 4H), 7.63 – 7.57 (m, 5H), 7.57 – 7.49 (m, 3H), 7.15 (t, *J* = 7.8 Hz, 9H), 2.28 (d, *J* = 6.6 Hz, 13H), 1.56 (d, *J* = 4.6 Hz, 19H). $^{13}C\{^{1}H\}$ NMR (125 MHz, $CDCl_3$) δ 142.96 – 141.04, 139.14, 138.16, 130.99, 130.08, 125.27, 121.30, 120.62, 118.43, 35.45, 31.85, 21.40. HRMS: Calculated mass $C_{34}H_{31}S_2O_2$ $[(M+H)^+]$ 535.1760; found 535.1752.

Synthesis of DSO_2

A Ccompound **(2)** (250 mg, 0.49 mmol, 1 eq) was dissolved in 20 ml of DCM at 0 °C. Subsequently *m*CPBA (55-75%, 422 mg, 2.45 mmol, 5 eq) added slowly to the mixture was stirred at 0 °C for 1 hours. Next the organic layer washed with brine (30 mL) and dried over anhydrous sodium sulphate. Then solvent was removed using rotary evaporation and crude product was purified by column chromatography using 50% DCM/Hexane as eluent gave green-yellow solid (224 mg, 88% yield). ^{1}H NMR (500 MHz, $CDCl_3$) δ 9.74 (s, 1H), 9.05 (d, J = 9.3 Hz, 2H), 8.38 (s, 2H), 8.33 (d, J = 9.4 Hz, 2H), 7.93 (d, J = 8.4 Hz, 4H), 7.30 – 7.23 (m, 4H), 2.33 (s, 6H), 1.54 (s, 9H). $^{13}C\{^{1}H\}$ NMR (125 MHz, $CDCl_3$) δ 151.36, 144.50, 138.84, 133.35, 132.23, 132.15, 130.05, 129.90, 128.15, 127.78, 126.55, 126.08, 122.73, 121.80, 35.50, 31.83, 21.70. IR (KBr) cm^{-1}: 3065, 2957, 2925, 2854, 1589, 1155, 1085, 664. HRMS: Calculated mass $C_{34}H_{30}O_4S_2Na$ $[(M+Na)^+]$ 589.1477; found 589.1491.

Photophysical studies

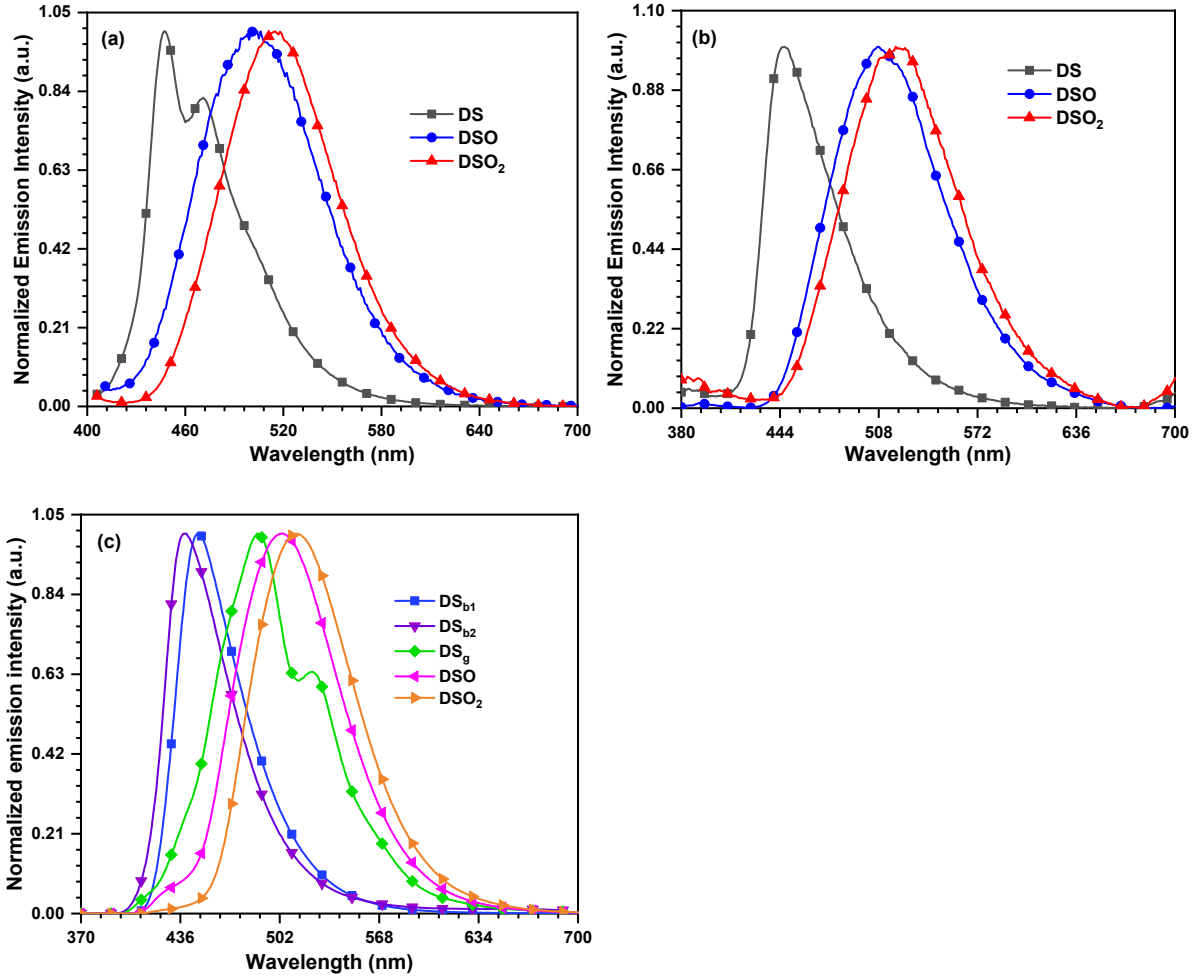

Fig. S1. (a) Emission spectra of all dyes in (a) thin film (λ_{ex} = 390 nm), (b) solid (λ_{ex} = 370 nm), and (c) crystal (λ_{ex} = 360 nm).

Table S1. Summary of photophysical properties.

Dye	λ_{max} (nm (ε_{max}, M^{-1} cm^{-1} × 10^3))[a]	λ_{em} (Sol[b] / film[c] / solid[d]) (nm) (Φ_{PL} % (Sol / film))[e]	Stokes shift (cm^{-1})	FWHM (Sol / film / solid)
DS	400, 382, 370 (36.80), 297, 287 (33.06), 248 (71.08)	430(0.13) / 478(0.56)/ 447	1077	52/ 57/ 53
DSO	375 (62.95), 358(52.43), 311, 289 (60.49), 278, 247 (84.86)	430(0.13) / 478(0.68)/ 507	3411	39/ 89/ 86

DSO_2	390 (63.80), 372(49.80), 293 (55.23), 283 (48.98), 260 (61.44), 249 (67.26)	410,430(0.53) / 527(0.74)/ 522	1192	45/ 82/ 86

a. Absorption measured in dichloromethane solution using 10^{-5} M.

b. Emission measured in dichloromethane solution using 10^{-6} M, c. thin film and d. solid.

e. Absolute photoluminescence quantum yields calculated by calibrated integrated sphere.

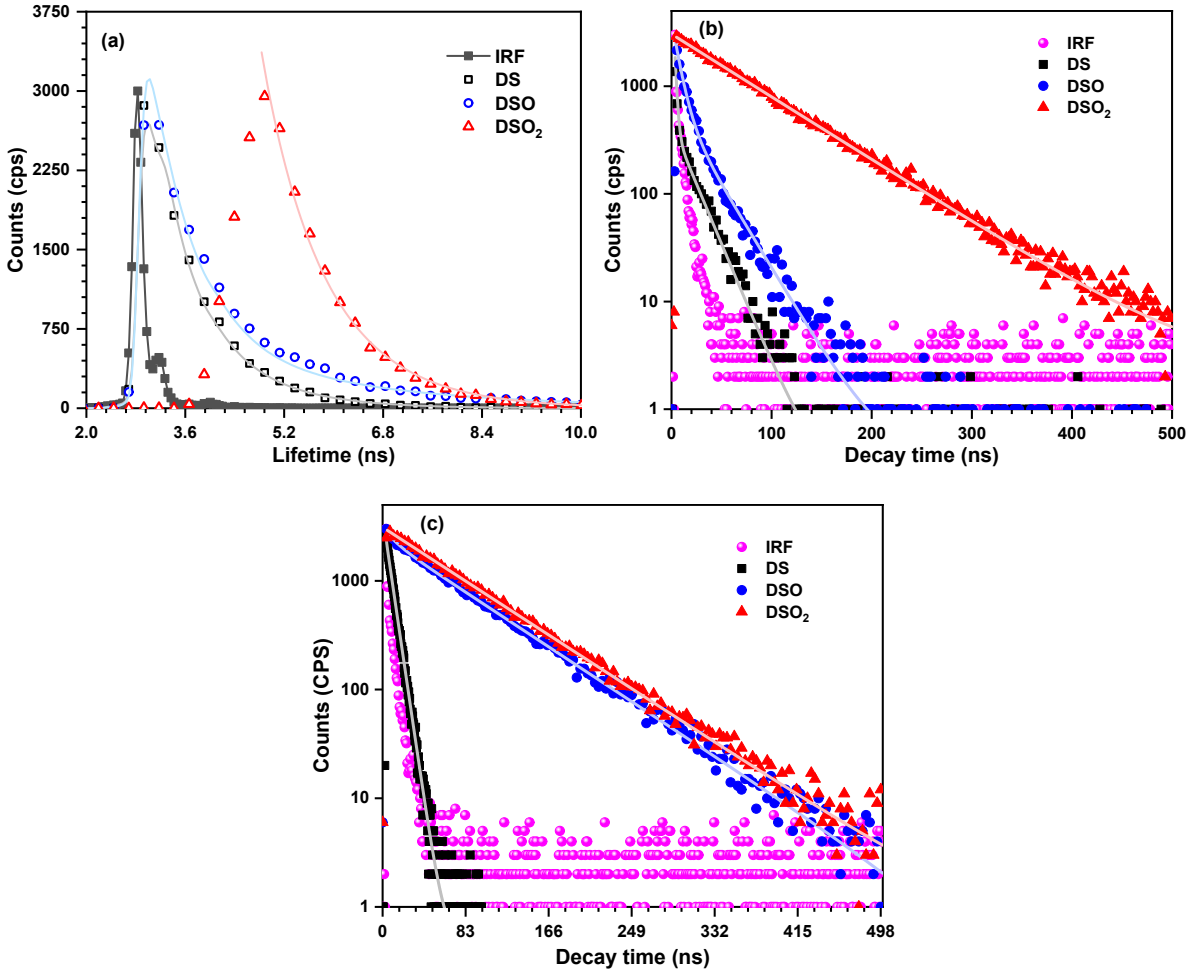

Figure S2. Lifetime decay of all dyes in (a) solution (b) thin film (c) solid.

Table S2. Lifetime decay of all dyes in solution, thin film and solid.

States	Dyes	τ_1 (ns)	τ_2 (ns)	Average τ (ns)	χ^2
Solution	**DS**	0.40	1.0	0.70	1.04
	DSO	0.65	2.75	1.61	0.96
	DSO_2	0.50	1.30	1.12	0.97
Thin film	**DS**	1.80	19.50	14.26	0.92
	DSO	7.0	28.0	18.60	0.90

	DSO_2	74.38	-	74.38	1.05
	DS	0.60	6.90	6.80	0.90
Solid	**DSO**	11.87	71.73	69.99	1.15
	DSO_2	72.75	-	72.75	1.10

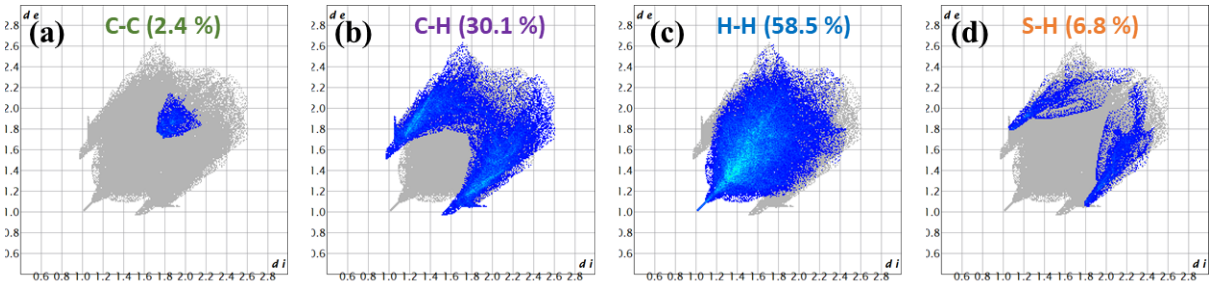

Figure S3. Decomposed Hirshfeld surface plots of **DS_{b2}** showing contributions from **(a) C···C, (b) C···H, (c) H···H** and **(d) S···H** interactions.

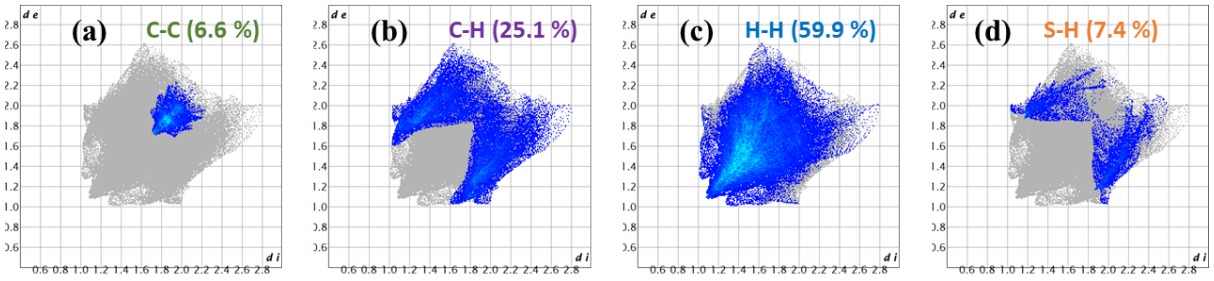

Figure S4. Decomposed Hirshfeld surface plots of **DS_g** showing contributions from **(a) C···C, (b) C···H, (c) H···H** and **(d) S···H** interactions.

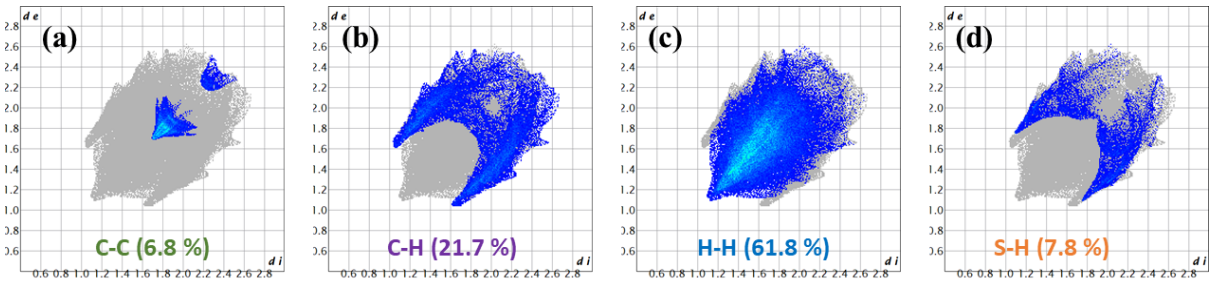

Figure S5. Decomposed Hirshfeld surface plots of **DS_{b1}** showing contributions from **(a) C···C, (b) C···H, (c) H···H** and **(d) S···H** interactions.

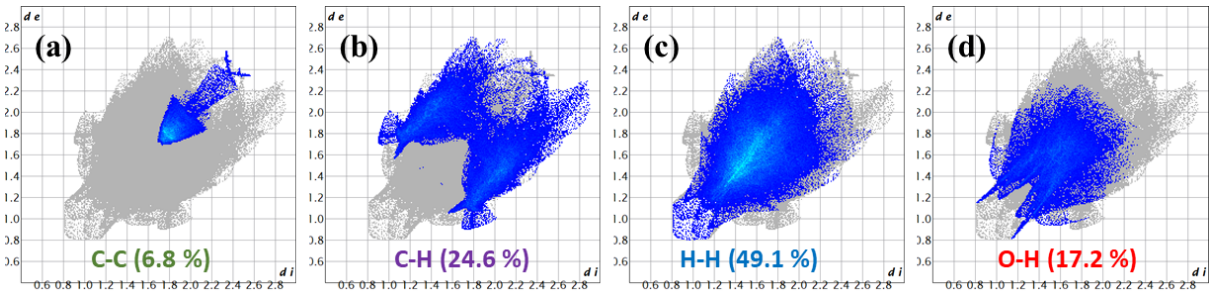

Figure S6. Decomposed Hirshfeld surface plots of **DSO** showing contributions from **(a) C···C**, **(b) C···H**, **(c) S···H,** and **(d) O···H** interactions.

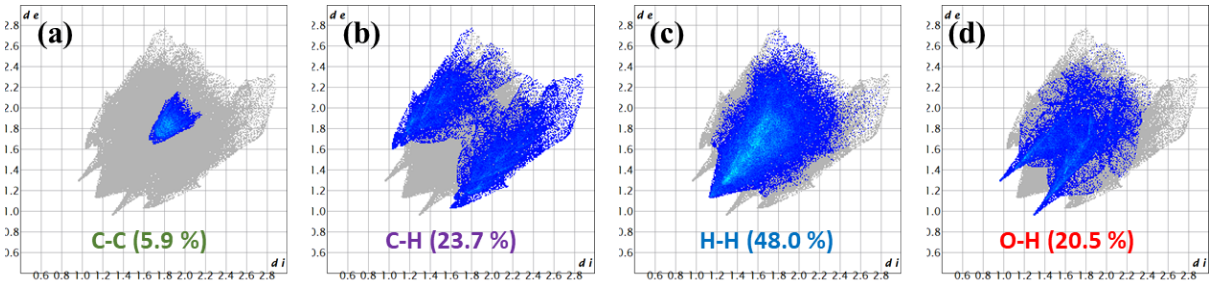

Figure S7. Decomposed Hirshfeld surface plots of **DSO_2** showing contributions from **(a) C···C**, **(b) C···H**, and **(c) O···H** interactions.

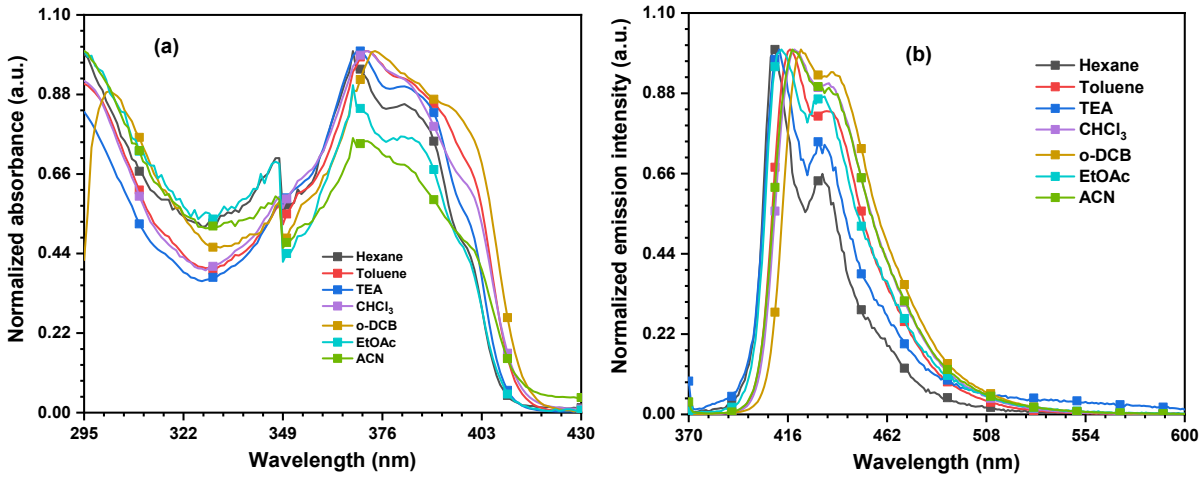

Fig. S8. (a) Absorption, (b) emission spectra of **DS** recorded in different solvents.

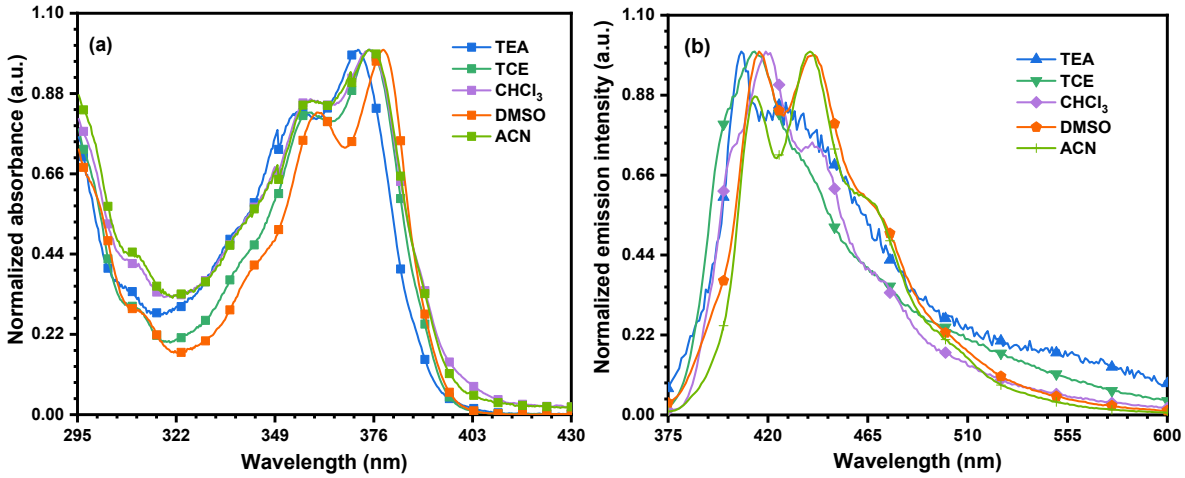

Fig. S9. (a) Absorption, (b) emission spectra of **DSO** recorded in different solvents.

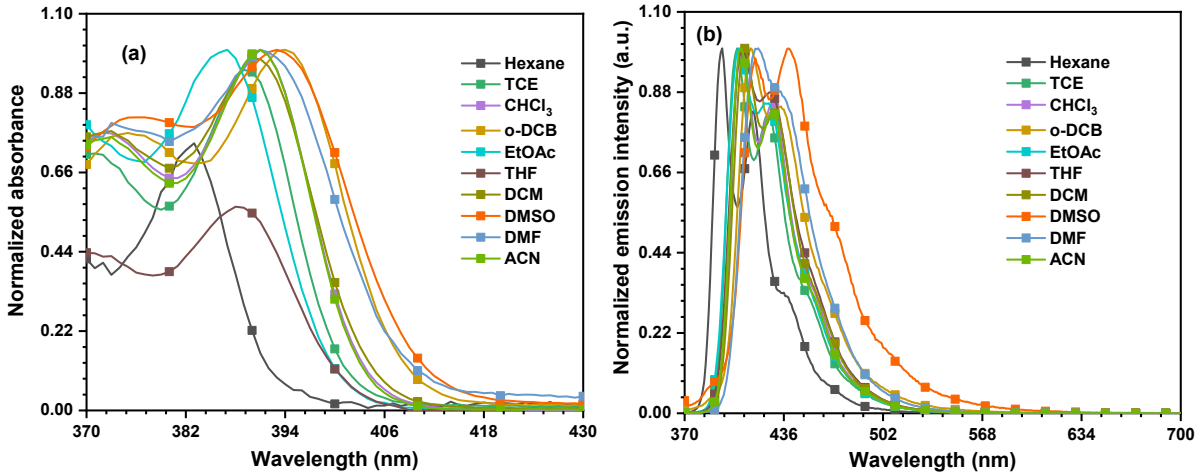

Fig. S10. (a) Absorption, (b) emission spectra of **DSO_2** recorded in different solvents.

Table S3. Solvatochromic data of **DS** in various solvents.

Solvent	E^N_T	Orientation Polarizability (Δf)	λ_{abs} (nm)	λ_{em} (nm)	Stokes Shift (nm)	Δν (cm^{-1})
Hex	0.009	0.012	368	409	2724.035	41
Tol	0.099	0.014	371	416	2915.716	45
TEA	0.043	0.045	369	411	2769.370	42
TCE	0.160	0.085	372	416	2843.258	44
***o*DCB**	0.225	0.186	371	419	3087.829	48
EtOAc	0.228	0.199	373	422	3112.969	49
ACN	0.460	0.305	368	419	3307.564	51

Table S4. Solvatochromic data of **DSO** in various solvents.

Solvent	E^N_T	Orientation Polarizability (Δf)	λ_{abs} (nm)	λ_{em} (nm)	Stokes Shift (nm)	Δν (cm^{-1})

Hex	0.009	0.012	371	408	2444.37398	37
TCE	0.160	0.085	374	414	2583.37854	40
$CHCl_3$	0.259	0.149	374	420	2928.4441	46
DMSO	0.444	0.263	378	440	3727.75373	62
ACN	0.460	0.305	375	439	3887.62339	64

Table S5. Solvatochromic data of **DSO_2** in various solvents.

Solvent	E^N_T	Orientation Polarizability (Δf)	λ_{abs} (nm)	λ_{em} (nm)	Stokes Shift (nm)	Δν (cm^{-1})
Hex	0.009	0.012	383	394	728.94991	11
TCE	0.160	0.085	390	407	1071.00107	17
$CHCl_3$	0.259	0.149	391	408	1065.64365	17
***o*DCB**	0.225	0.186	394	414	1226.12129	20
EtOAc	0.228	0.199	386	406	1276.19388	20
THF	0.207	0.210	389	408	1197.13695	19
DCM	0.309	0.217	390	409	1191.14789	19
DMSO	0.444	0.263	392	416	1471.74254	24
DMF	0.386	0.276	391	418	1652.00259	27

Table S6. Solvatochromic properties of all dyes.

Dye	Chemical formula	R^2	Onsager radius	Slope	Δμ
DS	$C_{34}H_{30}S_2$	0.90	4.69 A°	1929.9177	4.45 D
DSO	$C_{34}H_{30}O_2S_2$	0.99	4.75 A°	6005.23	8.06 D
DSO_2	$C_{34}H_{30}O_4S_2$	0.86	4.81 A°	2773.64	5.54 D

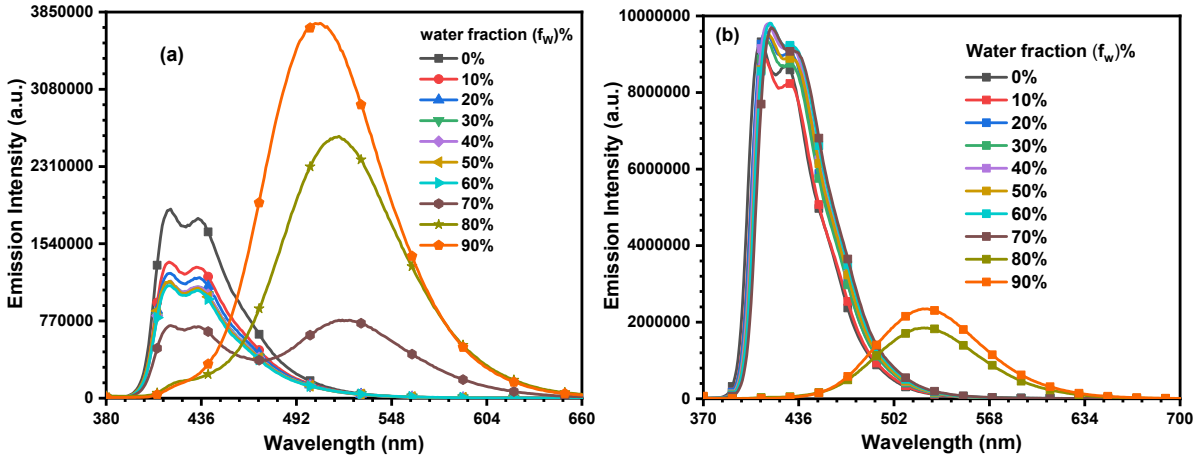

Figure S11. AIE study of (a) **DS** and (b) **DSO_2** in THF/H_2O mixture.

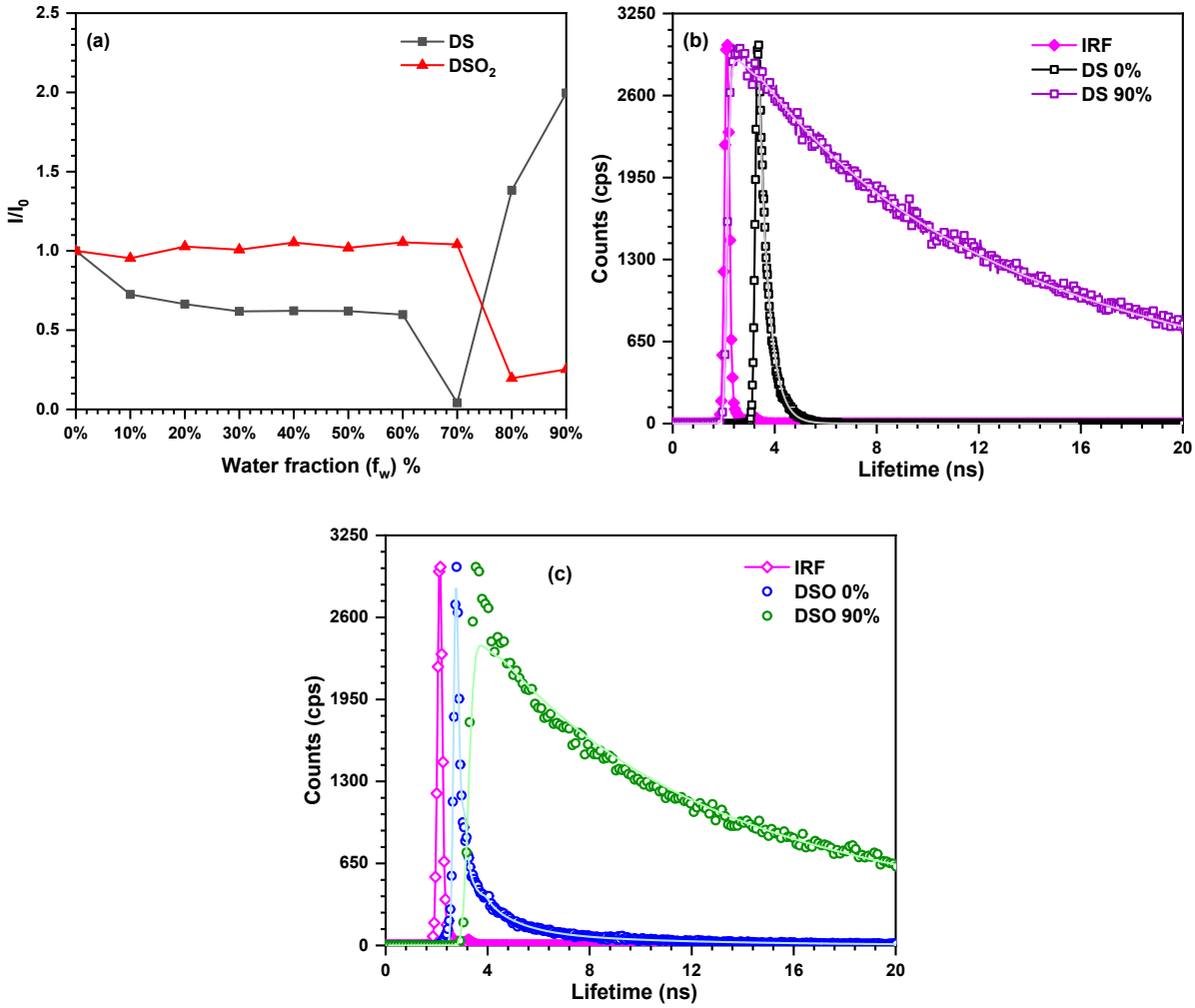

Figure S12. (a) I/I_0 plot of **DS** and **DSO_2**, Lifetime decay of (b) **DS,** (c) **DSO** in aggregated fractions.

Crystallographic data

Table S7. Selected bond lengths and angles observed in **DS**, **DSO** and **DSO_2**

Compound	C-S, Å	S=O, Å	C-S-C, °	C-S-C-C, °
DS_{b1}	1.7757(15)	-	101.90(7)	112.19(13)
	1.7763(15)		101.59(7)	-68.39(13)
DS_{b2}	1.7769(15)	-	102.97(7)	12.81(14)
	1.7752(15)		103.03(7)	21.37(14)
DS_g	1.7732(13)	-	106.43(6)	-11.79(12)
	1.7702(13)		103.65(6)	13.22(11)
DSO	1.457(3)	1.457(3)	97.25(6)	90.12(11)
	1.4853(12)	1.4853(12)	94.29(7)	-87.36
DSO_2	1.7807(16)	1.4398(13)	103.62(8)	92.68
	1.7740(17)	1.4388(13)	103.50(8)	-111.73

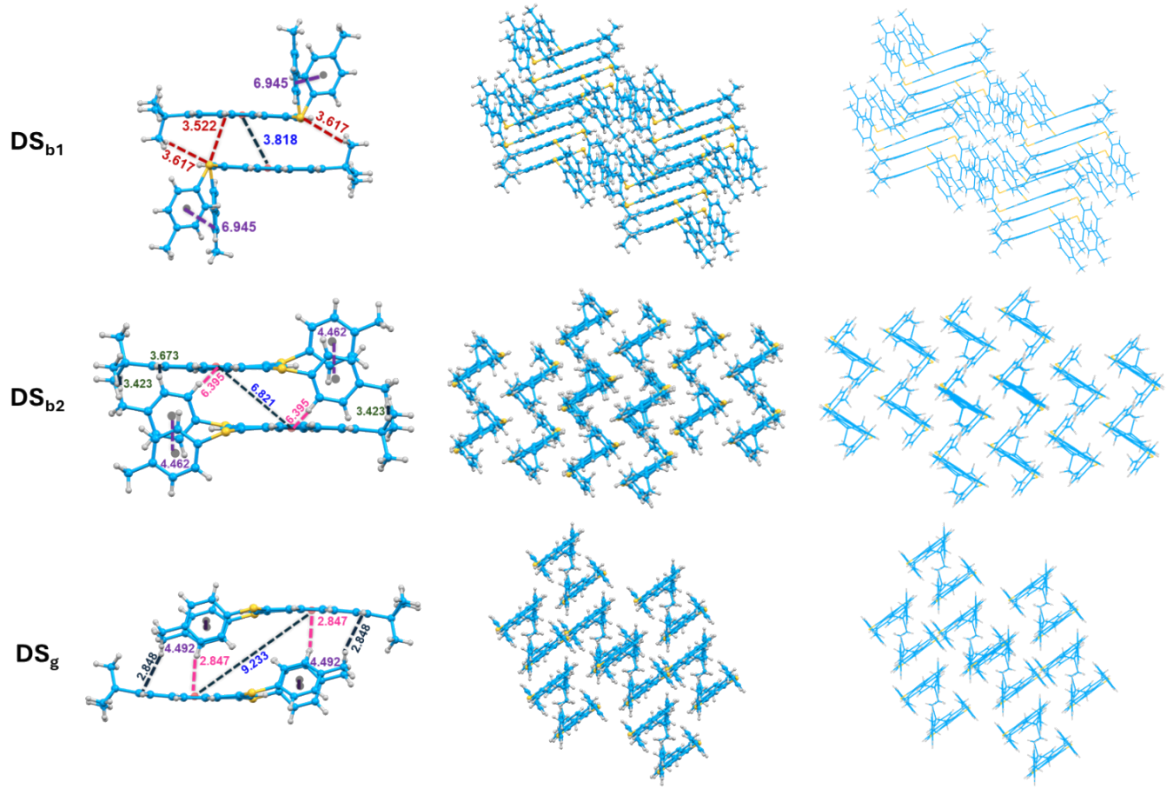

Figure S13. Packing analysis of **DS$_{b1}$**, **DS$_{b2}$**, and **DS$_g$** crystals.

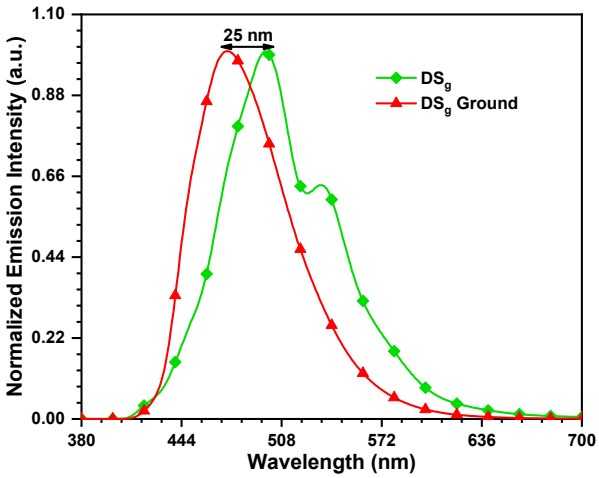

Figure S14. Emission spectrum of mechanochromic behaviour of **DS$_g$** crystal (λ_{ex} = 370 nm).

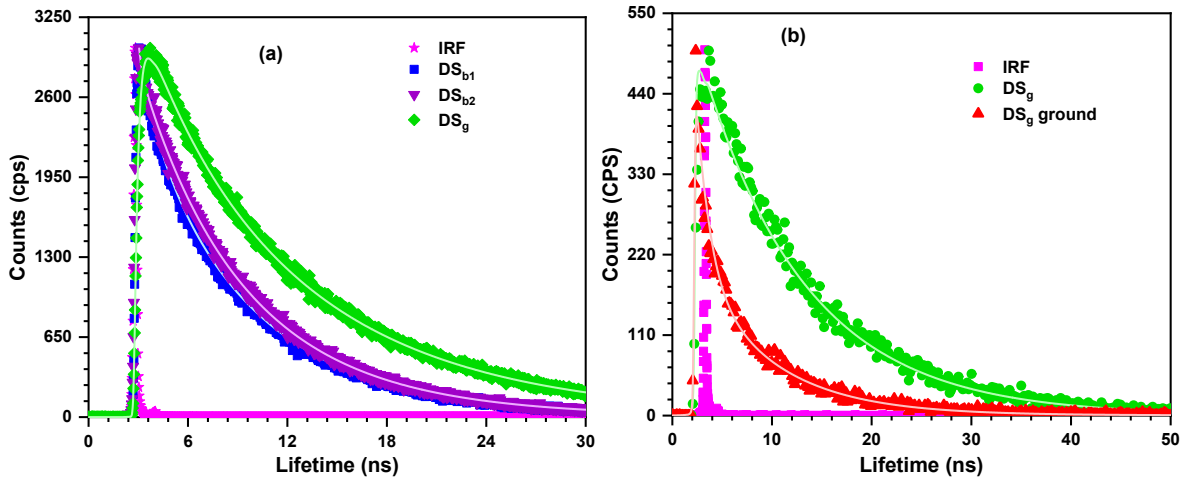

Figure S15. Lifetime decay of (a) **DS_{b1}**, **DS_{b2},** and **DS_g** crystals, (b) **DS_g** and **DS_g ground** crystals.

Table S8. Kinetic parameter of **DS** polymorph crystals.

Compound	PLQYs (%)	τ (ns)	k_r (s^{-1})	k_{nr} (s^{-1})
DS_{b1}	33.8	6.66	5.08 x 10^7	9.94 x 10^7
DS_{b2}	48.6	6.73	7.22 x 10^7	7.64 x 10^7
DSg	62.3	10.47	5.95 x 10^7	3.60 x 10^7

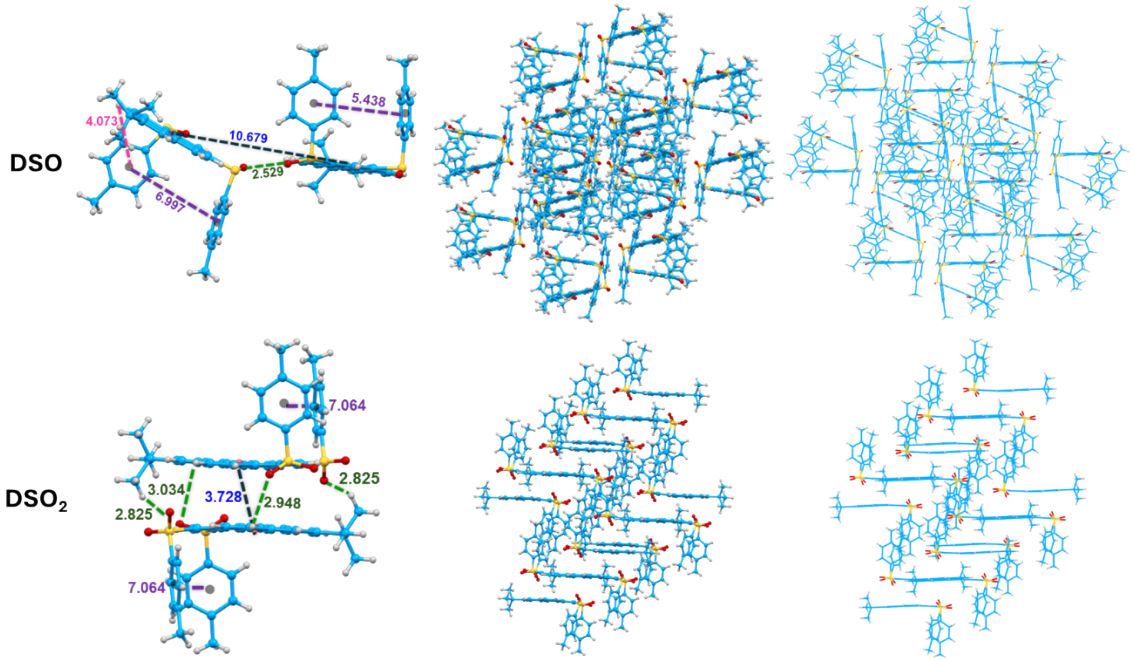

Figure S16. Packing analysis of **DSO,** and **DSO_2** crystals.

Theoretical studies

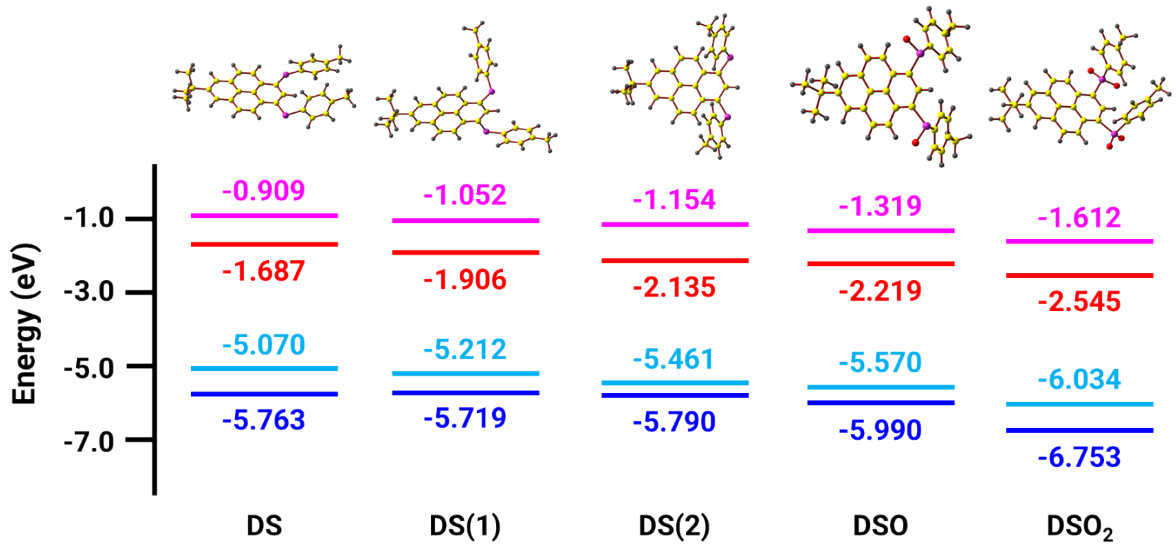

Figure S17. Frontier molecular orbital (FMOs) energy level of all dyes.

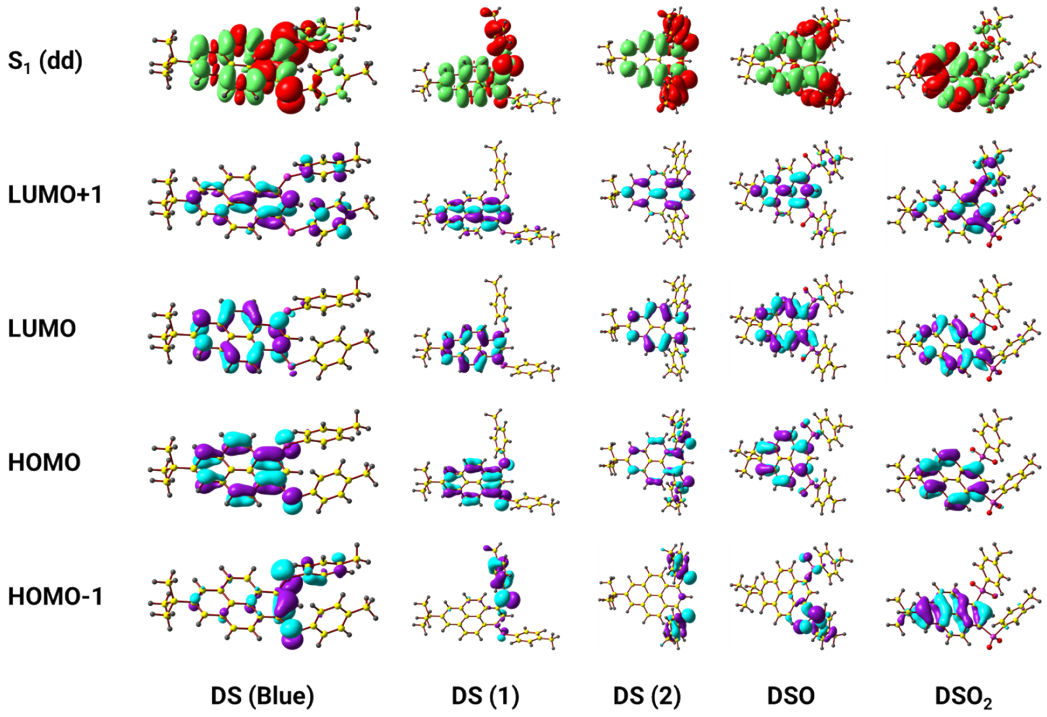

Figure S18. FMOs HOMO/HOMO-1 and LUMO/LUMO+1 electronic distributions and difference density plot for S_1 state of all dyes.

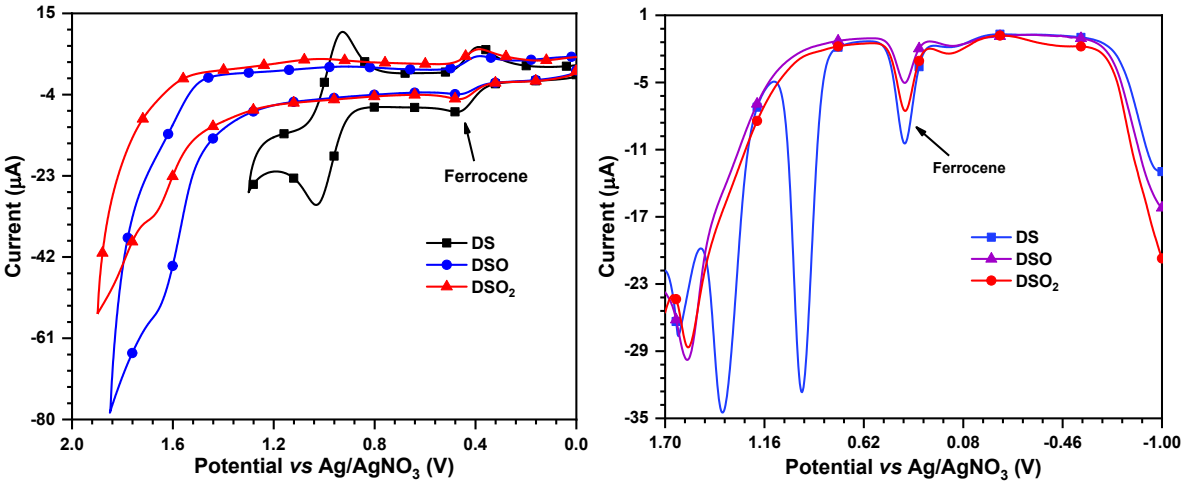

Figure S19. (a) Cyclic voltammetry and **(b)** DPV of all dyes recorded in DCM.

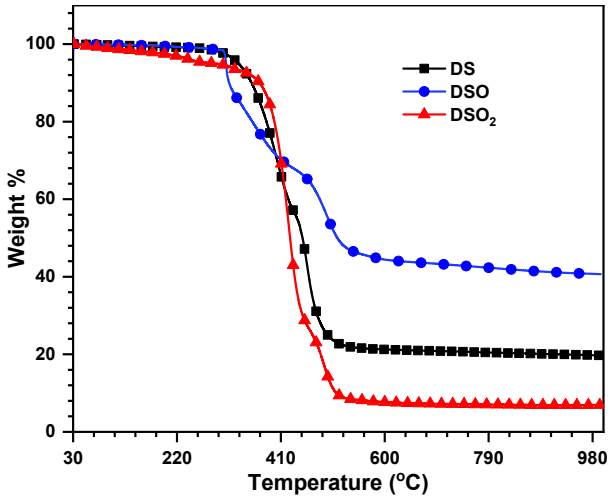

Figure S20. Thermal stability of all dyes.

Table S9. Thermal and electrochemical properties of all dyes.

Dye	E_{ox} (V)[a]	HOMO/LUMO (V)[b]	HOMO/LUMO (V)[c]	$E_{0\text{-}0}$ (V)[d]	T_{10d} (°C)[e]
DS	0.9563	-5.756/-2.604	-5.070/-1.687	393	353
DSO	1.5830	-6.383/-3.145	-5.570/-2.219	383	312
DSO_2	1.5713	-6.371/-3.260	-6.034/-2.545	398	375

a. Measured for 2 x 10^{-4} M DCM and the potentials are quoted with reference to ferrocene as internal standard.

b. HOMO = -(4.8 + E_{ox}), c. LUMO = HOMO – $E_{0\text{–}0}$.

c. HOMO and LUMO calculated by theory.

d. Optical band gap obtained from the intersection of absorption and emission spectra.

e. Temperature corresponding to 10% weight loss.

Table S10. Kinetic parameter of all dyes in various water fractions

Compound	Fraction	PLQYs (%)	τ (ns)	k_r (s^{-1})	k_{nr} (s^{-1})
DS	0% H_2O	18.09	0.3851	4.70×10^8	2.13×10^9
	99% THF/H_2O	50.50	15.2533	3.31×10^7	3.25×10^7
DSO	0% H_2O	14.25	2.8476	5.01×10^7	3.01×10^8
	99% THF/H_2O	76.77	19.4071	3.96×10^7	1.20×10^7

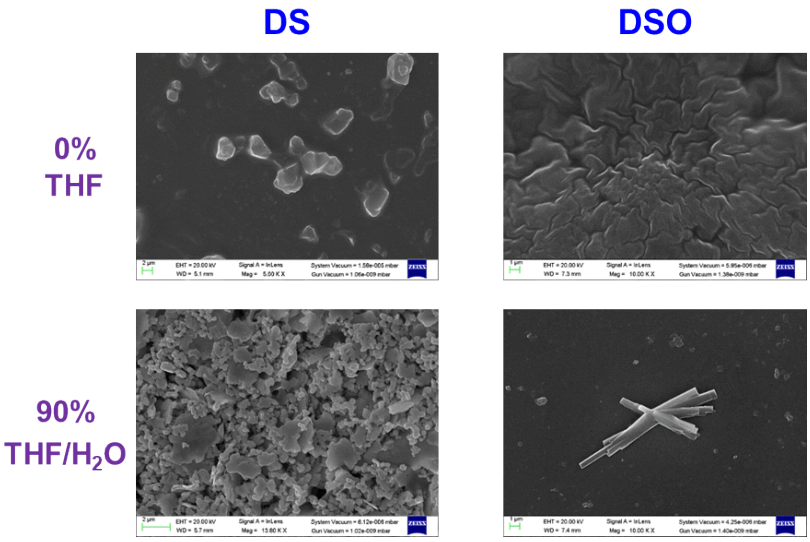

Figure S21. Solid state SEM images of all dyes.

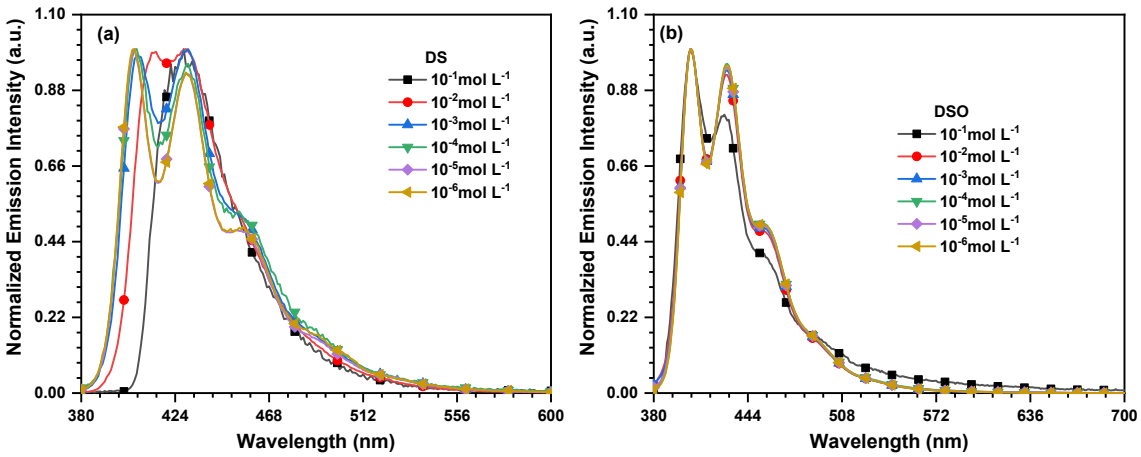

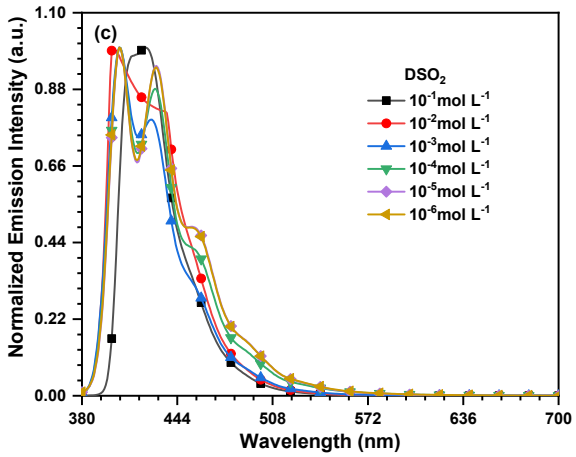

Figure S22. Concentration dependent emission of (a) **DS**, (b) **DSO**, and (c) **DSO_2**.

Table S11. Crystal data and structure refinement for **DS_{b1}**

CCDC No	2542598
Empirical formula	$C_{34}H_{30}S_2$
Formula weight	502.70
Temperature/K	100.0
Crystal system	triclinic
Space group	P-1
a/Å	9.6739(2)
b/Å	12.3529(2)
c/Å	12.9314(2)
α/°	118.4910(10)
β/°	98.7630(10)
γ/°	98.9760(10)
Volume/Å^3	1294.95(4)
Z	2
ρ_{calc}g/cm^3	1.289
μ/mm^{-1}	0.228
F(000)	532.0
Crystal size/mm^3	0.246 × 0.085 × 0.025
Radiation	MoKα (λ = 0.71073)
2Θ range for data collection/°	3.712 to 52.836
Index ranges	-12 ≤ h ≤ 12, -15 ≤ k ≤ 15, -16 ≤ l ≤ 16
Reflections collected	44318
Independent reflections	5309 [R_{int} = 0.0386, R_{sigma} = 0.0228]
Data/restraints/parameters	5309/0/330
Goodness-of-fit on F^2	1.180
Final R indexes [I>=2σ (I)]	R_1 = 0.0419, wR_2 = 0.1243
Final R indexes [all data]	R_1 = 0.0456, wR_2 = 0.1290
Largest diff. peak/hole / e Å^{-3}	0.48/-0.44

Table S12. Crystal data and structure refinement for **DS_{b2}**

CCDC No	2542596
Empirical formula	$C_{34}H_{30}S_2$
Formula weight	502.70
Temperature/K	150.00
Crystal system	triclinic
Space group	P-1
a/Å	9.8717(5)
b/Å	10.1637(5)
c/Å	14.9808(8)
α/°	93.7400(10)
β/°	93.3080(10)
γ/°	116.7710(10)
Volume/Å^3	1332.69(12)
Z	2
ρ_{calc}g/cm^3	1.253
μ/mm^{-1}	0.221
F(000)	532.0
Crystal size/mm^3	0.228 × 0.102 × 0.029
Radiation	MoKα (λ = 0.71073)
2Θ range for data collection/°	4.512 to 52.914
Index ranges	$-12 \le h \le 12$, $-12 \le k \le 12$, $-18 \le l \le 18$
Reflections collected	53734
Independent reflections	5489 [R_{int} = 0.0354, R_{sigma} = 0.0199]
Data/restraints/parameters	5489/0/330
Goodness-of-fit on F^2	1.041
Final R indexes [I>=2σ (I)]	R_1 = 0.0389, wR_2 = 0.1010
Final R indexes [all data]	R_1 = 0.0457, wR_2 = 0.1059
Largest diff. peak/hole / e Å^{-3}	0.30/-0.34

Table S13. Crystal data and structure refinement for **DS_g**

CCDC No	2542597
Empirical formula	$C_{34}H_{30}S_2$
Formula weight	502.7
Temperature/K	100(2)
Crystal system	triclinic
Space group	P-1
a/Å	9.8410(3)
b/Å	12.1021(4)
c/Å	12.1440(4)
α/°	65.1220(10)
β/°	88.5840(10)

γ/°	84.2020(10)
Volume/Å^3	1305.14(7)
Z	2
ρ_{calc}g/cm^3	1.279
μ/mm^{-1}	0.226
F(000)	532.0
Crystal size/mm^3	0.272 × 0.203 × 0.1
Radiation	Mo Kα (λ = 0.71073)
2Θ range for data collection/°	3.698 to 53.724
Index ranges	-12 ≤ h ≤ 12, -15 ≤ k ≤ 15, -15 ≤ l ≤ 15
Reflections collected	49182
Independent reflections	5588 [R_{int} = 0.0395, R_{sigma} = 0.0260]
Data/restraints/parameters	5588/78/361
Goodness-of-fit on F^2	1.038
Final R indexes [I>=2σ (I)]	R_1 = 0.0366, wR_2 = 0.1019
Final R indexes [all data]	R_1 = 0.0390, wR_2 = 0.1048
Largest diff. peak/hole / e Å^{-3}	0.32/-0.37

Table S14. Crystal data and structure refinement for **DSO**

CCDC No	2542600
Empirical formula	$C_{34}H_{30}O_2S_2$
Formula weight	534.70
Temperature/K	100.00
Crystal system	triclinic
Space group	P-1
a/Å	13.5813(12)
b/Å	13.7211(11)
c/Å	14.8971(13)
α/°	83.067(4)
β/°	77.368(4)
γ/°	85.922(4)
Volume/Å^3	2686.2(4)
Z	4
ρ_{calc}g/cm^3	1.322
μ/mm^{-1}	0.229
F(000)	1128.0
Crystal size/mm^3	0.4 × 0.353 × 0.23
Radiation	MoKα (λ = 0.71073)
2Θ range for data collection/°	3.076 to 63.896
Index ranges	-20 ≤ h ≤ 20, -20 ≤ k ≤ 20, -22 ≤ l ≤ 22
Reflections collected	154427
Independent reflections	18329 [R_{int} = 0.0839, R_{sigma} = 0.0529]
Data/restraints/parameters	18329/82/760

Goodness-of-fit on F^2	1.028
Final R indexes [I>=2σ (I)]	R_1 = 0.0499, wR_2 = 0.1157
Final R indexes [all data]	R_1 = 0.0737, wR_2 = 0.1318
Largest diff. peak/hole / e $Å^{-3}$	0.43/-0.41

Table S15. Crystal data and structure refinement for **DSO_2**

CCDC No	2542599
Empirical formula	$C_{34}H_{30}O_4S_2$
Formula weight	566.70
Temperature/K	103.0
Crystal system	triclinic
Space group	P-1
a/Å	9.7203(3)
b/Å	12.4319(3)
c/Å	13.7673(4)
α/°	71.5440(10)
β/°	70.8070(10)
γ/°	67.0850(10)
Volume/$Å^3$	1412.79(7)
Z	2
ρ_{calc}g/cm^3	1.332
μ/mm^{-1}	0.227
F(000)	596.0
Crystal size/mm^3	0.213 × 0.158 × 0.098
Radiation	MoKα (λ = 0.71073)
2Θ range for data collection/°	3.208 to 52.798
Index ranges	$-12 \le h \le 12$, $-15 \le k \le 15$, $-17 \le l \le 17$
Reflections collected	73288
Independent reflections	5801 [R_{int} = 0.0633, R_{sigma} = 0.0321]
Data/restraints/parameters	5801/0/366
Goodness-of-fit on F^2	1.037
Final R indexes [I>=2σ (I)]	R_1 = 0.0393, wR_2 = 0.1004
Final R indexes [all data]	R_1 = 0.0508, wR_2 = 0.1090
Largest diff. peak/hole / e $Å^{-3}$	0.32/-0.38

NMR Spectrum

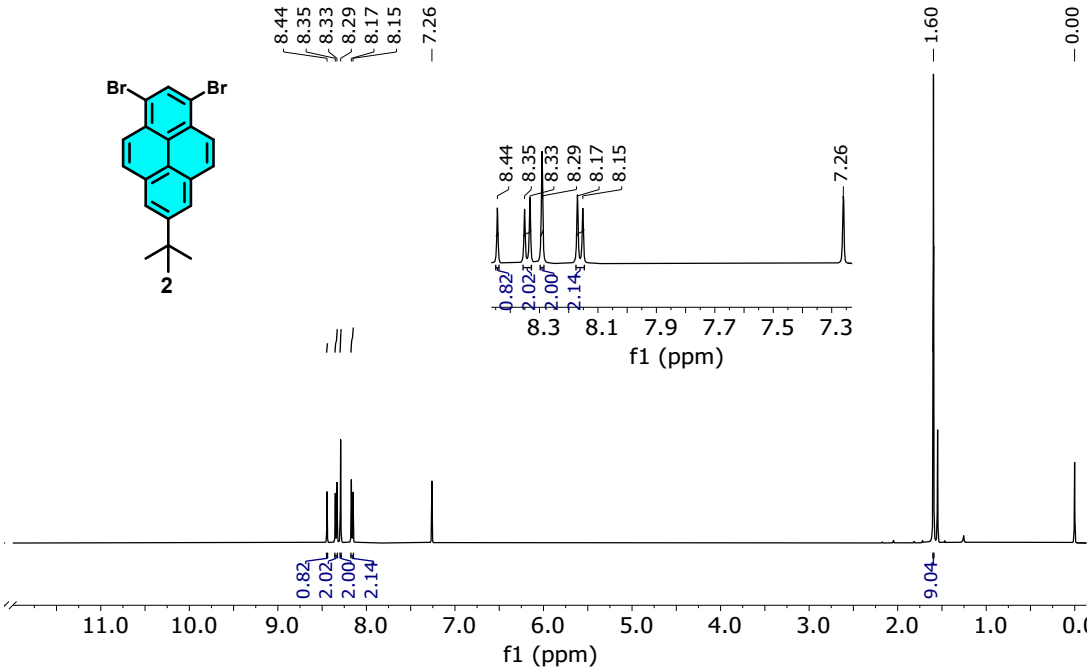

Figure S23. ^{1}H NMR (500 MHz, $CDCl_3$) of (**2**)

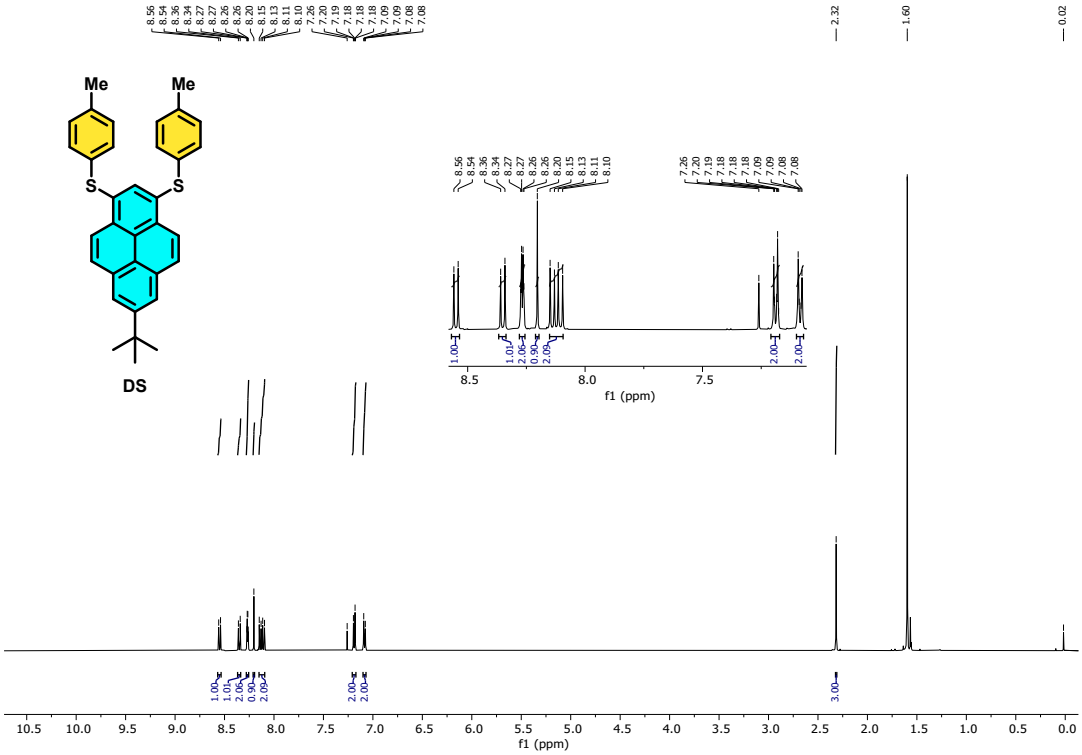

Figure S24. ^{1}H NMR (500 MHz, $CDCl_3$) of **DS**

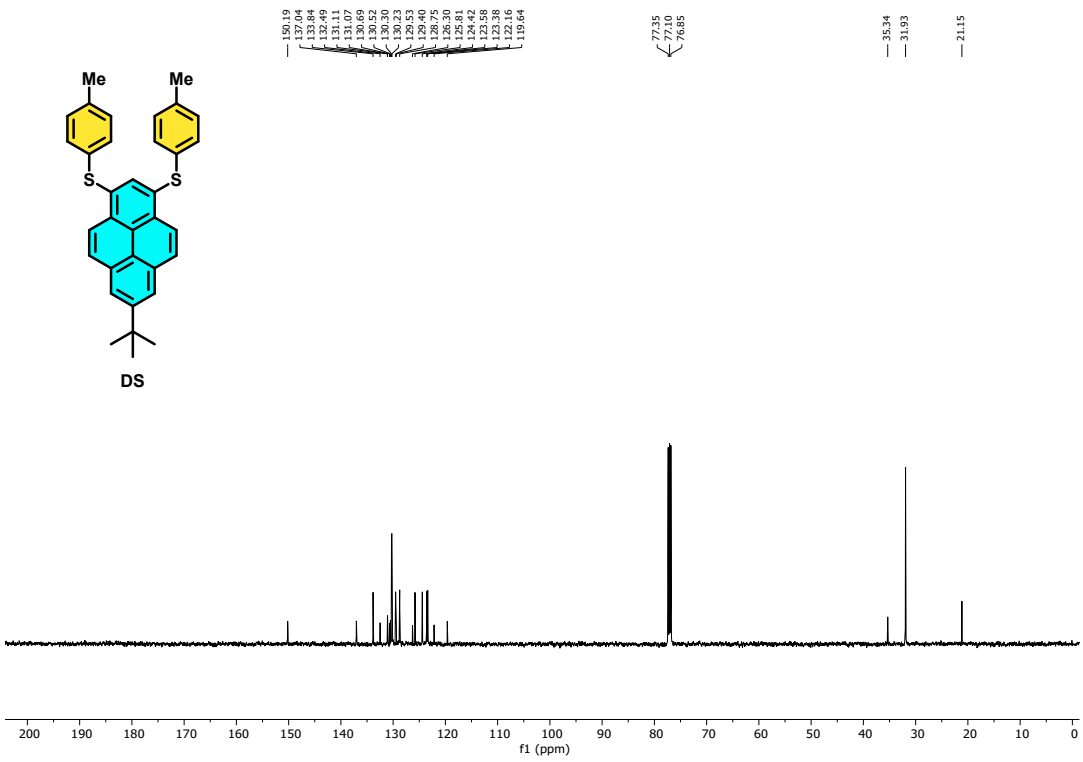

Figure S25. $^{13}C\{^{1}H\}$ NMR (125 MHz, $CDCl_3$) of **DS.**

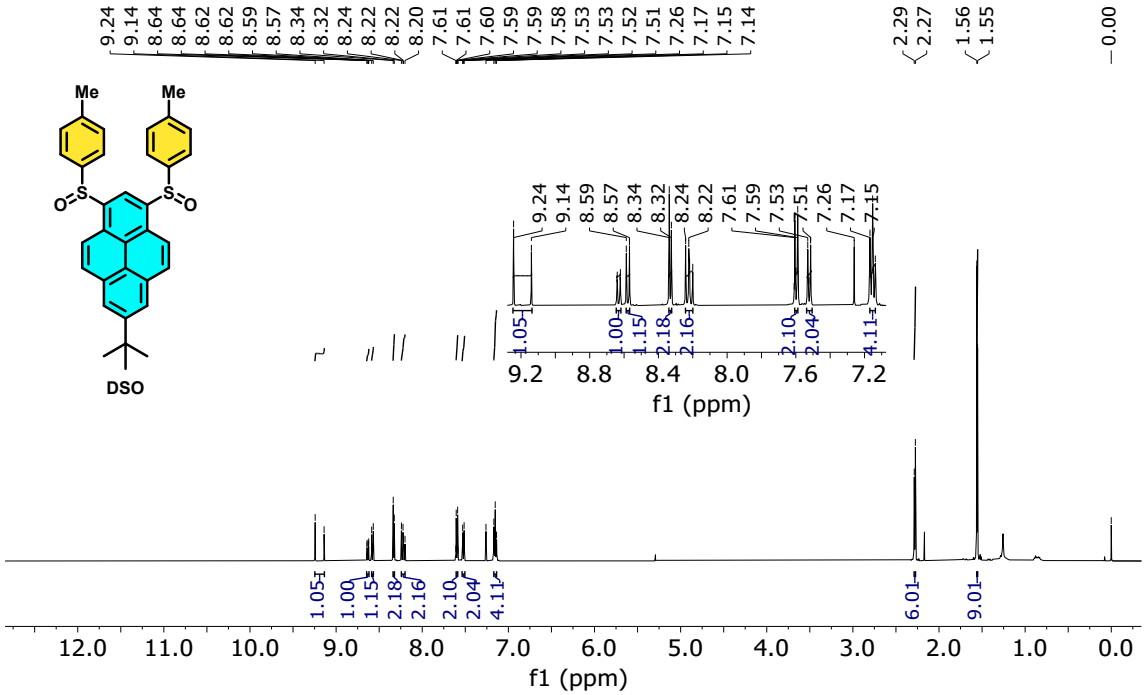

Figure S26. ^{1}H NMR (500 MHz, $CDCl_3$) of **DSO**

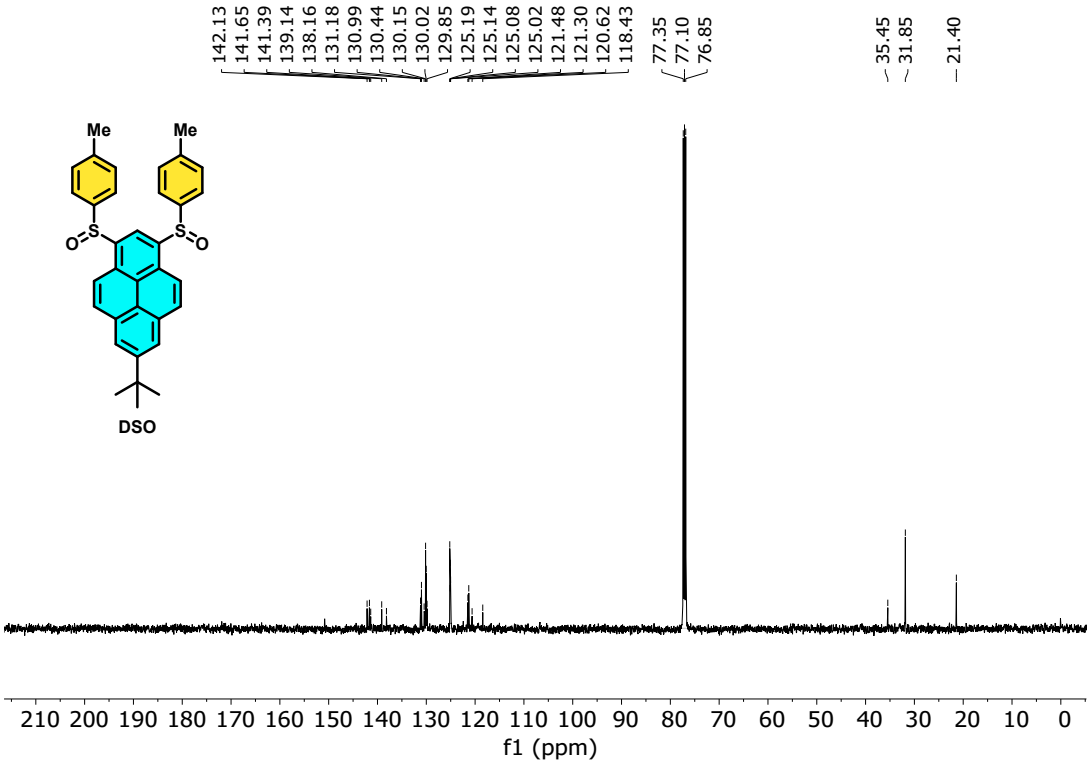

Figure S27. $^{13}C\{^{1}H\}$ NMR (125 MHz, $CDCl_3$) of **DSO**

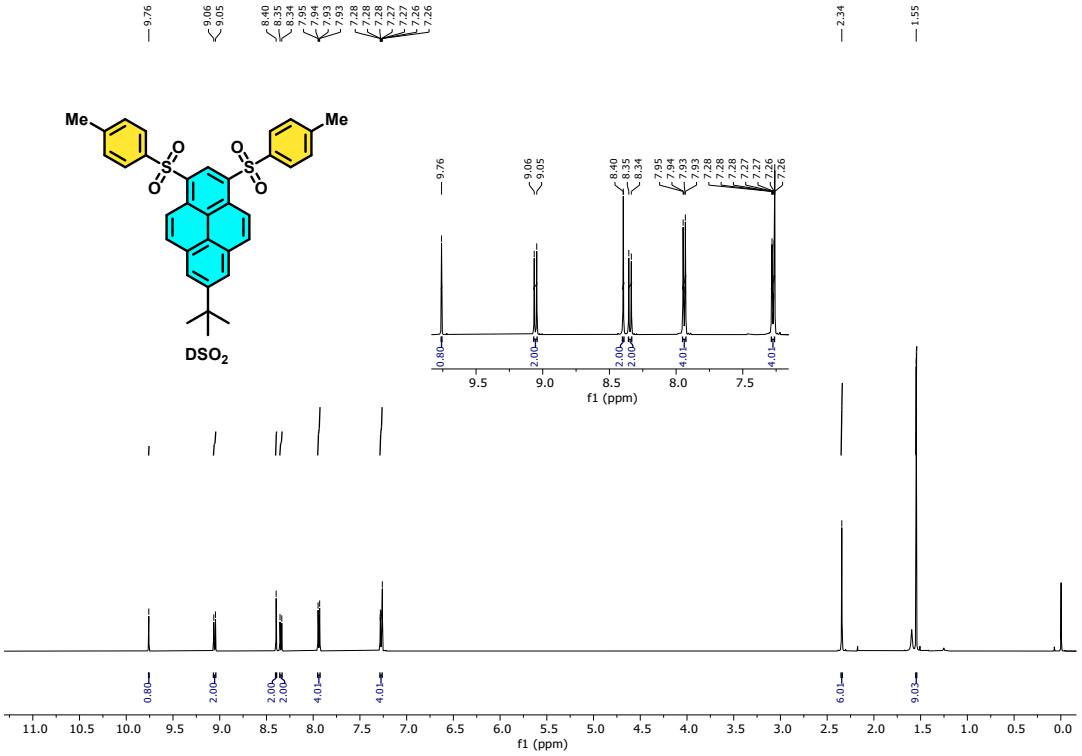

Figure S28. ^{1}H NMR (500 MHz, $CDCl_3$) of **DSO_2**

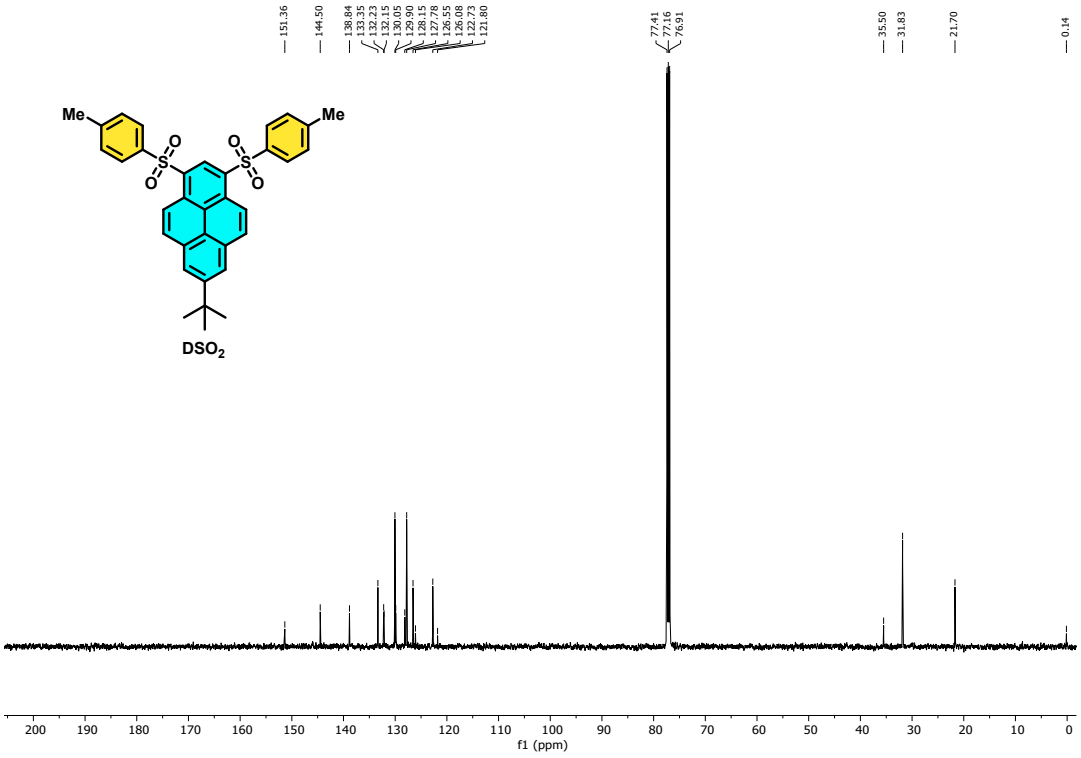

Figure S29. $^{13}C\{^{1}H\}$ NMR (125 MHz, $CDCl_3$) of **DSO_2**

References

1. F. Neese, *Wiley Interdiscip. Rev.: Comput. Mol. Sci*., 2025, **15**, 2, e70019.
2. T. Lu, *J. Chem. Phys.*, 2024, **161**, e082503.
3. A. Karuppusamy, T. Vandana and P. Kannan, *Journal of Photochemistry and Photobiology A: Chemistry*, 2017, **345**, 11-20.
4. L. Djordjevic, C. Valentini, N. Demitri, C. Meziere, M. Allain, M. Salle, A. Folli, D. Murphy, S. Manas-Valero, E. Coronado, D. Bonifazi, *Angew. Chem., Int. Ed.*, 2020, ***59***, 4106-4114.
5. J. Han, L. Wang, Y. Zhang, Y. Li, J. Wang, *Org. Lett.* 2021, **23**, 8688-8693.